Eur J Nucl Med Mol Imaging (2011) 38:2219–2227
DOI 10.1007/s00259-011-1882-1

ORIGINAL ARTICLE

Functional implications of hippocampal degeneration in early Alzheimer's disease: a combined DTI and PET study

Igor Yakushev · Matthias Schreckenberger · Matthias J. Müller · Ingrid Schermuly · Paul Cumming · Peter Stoeter · Alex Gerhard · Andreas Fellgiebel

Received: 28 March 2011 / Accepted: 3 July 2011 / Published online: 27 July 2011

Abstract
Purpose Hypometabolism of the posterior cingulate cortex (PCC) in early Alzheimer's disease (AD) is thought to arise in part due to AD-specific neuronal damage to the hippocampal formation. Here, we explored the association between microstructural alterations within the hippocampus and whole-brain glucose metabolism in subjects with AD, also in relation to episodic memory impairment.
Methods Twenty patients with early AD (Mini-Mental State Examination 25.7±1.7) were studied with [^{18}F]fluorodeoxyglucose (FDG) positron emission tomography and diffusion tensor imaging. Episodic memory performance was assessed using the free delayed verbal recall task (DVR). Voxel-wise relative FDG uptake was correlated to diffusivity indices of the hippocampus, followed by extraction of FDG uptake values from significant clusters. Linear regression analysis was performed to test for unique contributions of diffusivity and metabolic indices in the prediction of memory function.
Results Diffusivity in the left anterior hippocampus negatively correlated with FDG uptake primarily in the left anterior hippocampus, parahippocampal gyrus and the PCC ($p<0.005$). The same correlation pattern was found for right hippocampal diffusivity ($p<0.05$). In linear regression analysis, left anterior hippocampal diffusivity and FDG uptake from the PCC cluster were the only significant predictors for performance on DVR, together explaining 60.6% of the variance. We found an inverse association between anterior hippocampal diffusivity and PCC glucose metabolism, which was in turn strongly related to episodic memory performance in subjects with early AD.
Conclusion These findings support the diaschisis hypothesis of AD and implicate a dysfunction of structures along the hippocampal output pathways as a significant contributor to the genesis of episodic memory impairment.

Keywords Diffusion tensor imaging · Positron emission tomography · Episodic memory · Dementia · Mild cognitive impairment · Posterior cingulate

I. Yakushev (✉) · M. J. Müller · I. Schermuly · A. Gerhard · A. Fellgiebel
Department of Psychiatry and Psychotherapy,
University Medical Center Mainz,
Untere Zahlbacher Str. 8,
55131 Mainz, Germany
e-mail: igor.yakushev@uni-mainz.de

M. Schreckenberger
Department of Nuclear Medicine,
University Medical Center Mainz,
Mainz, Germany

P. Stoeter
Institute of Neuroradiology, University Medical Center Mainz,
Mainz, Germany

P. Cumming
Department of Nuclear Medicine, University of Munich,
Munich, Germany

A. Gerhard
Wolfson Molecular Imaging Centre, University of Manchester,
Manchester, UK

Introduction

The hippocampus and adjacent entorhinal cortex are the sites of earliest deposition of hyperphosphorylated tau protein filaments in cases of Alzheimer's disease (AD) [1]. This initial pathology is assumed to subserve the declaration of episodic memory impairment, which is the earliest and arguably the most severe clinical deficit in most patients with AD [2]. In accordance with findings of

postmortem neuropathological studies, a large body of magnetic resonance imaging (MRI) investigations have consistently documented reduction in hippocampal volume at early stages of AD (for a review see [3]). In contrast, functional imaging studies with positron emission tomography (PET) and single photon emission computed tomography (SPECT) reported the posterior cingulate cortex (PCC) to be the most common site of the earliest metabolic and perfusion deficits in AD [4, 5]. Furthermore, the extent of metabolic impairment in the PCC cannot be attributed to local atrophy, even in cases of frank dementia [6]. The most common hypothesis to explain this discrepancy is that hypometabolism/hypoperfusion of the PCC, at least in part, arises as a remote effect of AD-specific neuronal damage to the hippocampal formation [4, 7].

Indirect evidence for the so-called diaschisis hypothesis is provided by animal studies, which have shown the presence of dense reciprocal connections between the hippocampal formation and the PCC [8, 9]. These projections, which are dominated by fibres of the cingulate bundle, could be also identified in vivo in humans using the noninvasive MR-based technique of fibre tracking [10]. Notably, neurotoxic lesions of the hippocampal formation lead to posterior cingulate hypometabolism in nonhuman primates [7, 11].

Only very recently, in vivo human imaging studies have provided some direct support for the diaschisis hypothesis of AD. In a cross-modal imaging study, Villain and colleagues [12] found that hippocampal atrophy in AD patients was specifically related to disruption of white matter including the cingulate bundle, which in turn significantly correlated with the normalized uptake of [^{18}F]fluorodeoxyglucose (FDG) in the PCC, as well as parts of the classic Papez circuit [13]. In addition, Guedj and coworkers [14] reported a positive correlation between hippocampal volume and perfusion of the PCC in patients with amnestic mild cognitive impairment (aMCI), who run a high risk of proceeding to Alzheimer's dementia [15]. However, neither of these studies explored the association of neuroimaging parameters with cognitive performance, and it remained unknown if the disclosed structural-metabolic/structural-perfusion relationships had indeed any functional implications, in particular with respect to episodic memory. Furthermore, AD-related degeneration of the hippocampus associated with regional metabolism/perfusion has so far been probed only at the macroscopic level, i.e. in terms of volume reduction [12, 14].

Recent advances in the field of MRI have allowed quantitative assessment of brain tissue integrity at the microstructural level. Diffusion tensor imaging (DTI), a relatively new MRI-based technique for mapping the diffusion properties of water [16], is sensitive to subtle differences in the architecture of tissue. Indeed, DTI parameters were reported to have comparable or even greater diagnostic utility than do ordinary volumetric measures in MCI and AD [17–19]. Using these methods, we have recently shown that microstructural changes in the hippocampus were considerably more predictive than were ordinary volumetric indices of the extent of functionally relevant degeneration in patients with early AD, as manifest in impaired episodic memory [20].

Here, we contend that combining two in vivo imaging modalities, PET and DTI, in conjunction with cognitive testing can offer novel insights into the diaschisis hypothesis of AD. In an extension of our previous report, we used FDG PET to investigate what local or remote metabolic changes are associated with regional microstructural alterations of the hippocampus in a well-characterized group of patients with early AD [20], and then sought to relate the observed metabolic pattern with episodic memory.

Materials and methods

Subjects and design

From a prospective DTI study, we retrospectively selected subjects with early AD who had undergone clinical psychiatric and neurological examinations, laboratory tests (vitamin B_{12}, thyroid hormones, folate), FDG PET and MRI examinations according to the protocol reported below. As previously [20], early AD was diagnosed on the basis of history of progressive cognitive decline over at least 6 months, presenting with memory impairment, a Clinical Dementia Rating (CDR) of 0.5 or 1.0, a score on the Mini-Mental State Examination (MMSE) of at least 23 points and an "Alzheimer-typical" finding for FDG PET [21] as supportive biological marker [22]. Exclusion criteria were a history or presence of other organic brain diseases, substance abuse, any psychiatric diagnoses other than dementia, diabetes mellitus and evidence of leucoencephalopathy on T2- and fluid-attenuated inversion recovery (FLAIR)-weighted MR images. These criteria were fulfilled by 20 right-handed patients, of whom 15 had CDR 0.5 and 5 had CDR 1.0. The group included 16 men and 4 women, aged 69.8±7.4 years (mean±SD), with 13.3±2.1 years of education, and who had an MMSE score of 25.7±1.7 points. Cognitive evaluation was based on the German version of the Consortium to Establish a Registry of Alzheimer's Disease (CERAD) battery [23]. The free delayed verbal recall test (DVR) was used to assess episodic memory performance. The local Ethics Committee approved the study, to which all participants gave their written informed consent.

MR data acquisition

Clinical, neuropsychological exams, MRI/DTI and PET examinations were performed within a few days of each other. Data were obtained on a Siemens Magnetom Sonata 1.5 T system with gradients of 40 mT/m using a parallel imaging technique [8-channel iPAT coil and a generalized autocalibrating partially parallel acquisitions (GRAPPA) reconstruction algorithm], which reduces the number of phase-encoding steps during the image acquisition, susceptibility artefacts and spatial distortion inherent to DTI based on single-shot echo planar imaging (EPI) sequences. Acquisitions included 3-D magnetization prepared rapid acquisition gradient echo (MPRAGE) data sets with a 1 mm^3 isotropic voxel size, proton density (PD)/T2-weighted and FLAIR sequences (for parameters see [20]). The DTI data were acquired as transversal diffusion-weighted EPI sequences with 6 gradient directions [repetition time (TR)/echo time (TE)=8,000/105 ms, b=0 and 1,000 s/mm^2, matrix 128×128, slice thickness 3 mm without gap, voxel size 1.8×1.8×3.0 mm and 6 averages]. Scans with severe motion artefacts were excluded.

DTI data post-processing

Diffusion tensors (D) were computed by fitting the model to the signal intensities measured with the above-mentioned DTI imaging sequence [24]. The decomposition of D into its eigenvalues (λ1, λ2, λ3) and eigenvectors (ε1, ε2, ε3) was accomplished by symmetric bi-diagonalization followed by QR reduction routines as implemented in GNU Scientific Library (version 1.13, http://www.gnu.org/software/gsl). Mean diffusivity (MD) was calculated as the mean of the eigenvalues of the diffusion tensor [(λ1+λ2+λ3)/3], with units of mm^2/s [2] and presented as voxel-wise MD index maps.

Hippocampal diffusivity

Hippocampal diffusivity was sampled using a region of interest (ROI) analysis as implemented in Analyze® Software (Version 8.1; Biomedical Imaging Software System) [20]. To minimize contamination from cerebrospinal fluid (CSF) signal, uniform ROIs of 3×3 mm were manually placed on three consecutive slices of the individual MPRAGE image. For anterior measurements (Fig. 1), these ROIs comprised the three most anterior slices of the hippocampal volume, as previously defined (see Fig. 1 in [20]). For posterior measurements, which served as reference, the ROIs comprised the three most posterior slices of the hippocampal volume. Intra-rater reliability was assessed in a subset of 20 randomly selected subjects, 10 patients and 10 controls with the rater being blind to the subjects' status. The intra-class correlation coefficients were above 0.85 (0.86–0.92) for all ROIs. Then, individual MD and high-resolution T1-weighted MPRAGE images were coregistered using a mutual information 3-D rigid-body coregistration algorithm implemented in SPM5 (www.fil.ion.ucl.ac.uk/spm). The ROI sets were transferred to the respective MD images, and the mean magnitudes for anterior and posterior hippocampus were calculated separately for each hemisphere.

PET data acquisition and preprocessing

The protocol of data acquisition has been described in detail previously [25]. In brief, PET scans were acquired under standard resting conditions, using a Siemens ECAT EXACT scanner (CTI, Knoxville, TN, USA) in 3-D mode. The PET apparatus has an axial field of view of 16.2 cm in 47 planes and an axial resolution of ~6.0 mm full-width at half-maximum (FWHM). Thirty minutes after injection of FDG, a sequence of three 5-min frames was initiated, and later (after control for motion between frames) combined into a single frame. After correction for scatter, dead time and attenuation, emission images were reconstructed by filtered backprojection using a 4-mm Hamming filter.

Image analysis was performed using SPM5, implemented in MATLAB 6.5 (MathWorks Inc., Sherborn, MA, USA). The FDG uptake images were spatially normalized using an in-house tracer-, scanner- and age-specific brain PET template [in Montreal Neurological Institute (MNI) space] based on FDG recordings from ten healthy elderly subjects [26]. Spatially normalized images were represented in a 91×109×91 matrix with voxels measuring 2×2×

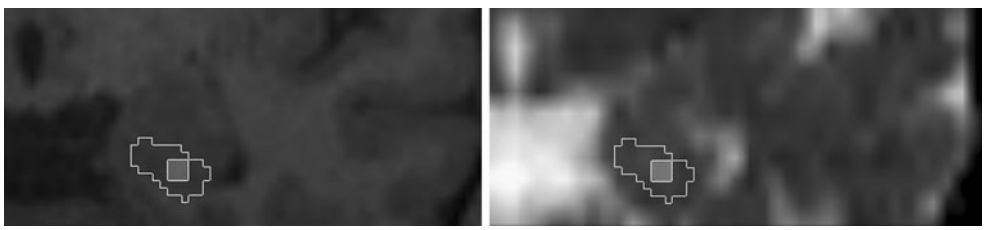

Fig. 1 Regions of interest (*white square*) for anterior diffusivity measurements were defined within the most anterior three slices of the predefined hippocampal volume of interest (*white polygon*) on coronal MR images (*left image*) and were transferred to corresponding coregistered MD images (*right image*)

2 mm, and then smoothed with a Gaussian filter of 12 mm FWHM. Finally, the FDG uptake maps were intensity normalized using the reference cluster approach as described in detail previously [26].

Statistical analysis

Raw scores in the DVR test were converted to standardized scores (z scores) using the population mean and standard deviation, adjusted for age, sex and education [23].

As diffusivity measurements did not deviate significantly from normal distribution ($p>0.10$ in Kolmogorov-Smirnov test), a parametric voxel-wise statistical analysis implemented in SPM5 was utilized. Relative FDG uptake in each brain voxel was correlated to diffusivity measurements in the hippocampus, with age, gender and education treated as nuisance variables. The SPM analyses generated a voxel-wise t statistic, comprising a statistical parametric map (SPM_t) for each contrast. A significance threshold was set at $p<0.005$ uncorrected for multiple comparisons, and a threshold for minimum spatial extent of 30 contiguous voxels was applied. After conversion of the MNI coordinates to the Talairach coordinates by a nonlinear transform (http://imaging.mrc-cbu.cam.ac.uk/imaging/MniTalairach), the anatomical localizations of peak clusters were identified using the Talairach Demon Client, v2.4 (http://www.talairach.org/client.html).

To examine if the established relationships have any implications in respect of memory function, the following analyses were performed. Using MarsBaR for SPM (http://marsbar.sourceforge.net/), we extracted individual relative FDG uptake values from all significant clusters of the SPM analysis. Afterwards, these values, as well as hippocampal diffusivity measurements (right and left anterior, right and left posterior), were correlated to DVR scores. Finally, all the above diffusivity and metabolic measurements (independent variables) were subjected into a stepwise linear regression analysis to test for their unique contributions in the prediction of performance on DVR (dependent variable).

As significant effects in voxel-based analyses are typically found at a subregional level, we in addition extracted FDG uptake from the entire anatomical regions, within which clusters of the above SPM analyses were located. This was done to examine the specificity of the potential relationships, i.e. whether FDG uptake from the clusters (which correlated with hippocampal diffusivity) rather than from the corresponding (entire) structures is stronger associated with performance on DVR. This volume of interest (VOI) analysis was performed using a probabilistic atlas of the brain [27, 28] as described in detail elsewhere [29]. Intensity scaling was identical for cluster- and VOI-based measurements.

The statistical tests were performed using SPSS software package version 18.0 (SPSS Inc., Chicago, IL, USA).

Results

Neuropsychological performance, volumetric and diffusivity measurements in this cohort have been reported in detail previously [20]. In brief, patients performed less well than controls in all cognitive tests, including the DVR ($p<0.001$). Among diffusivity measures, diffusivity of the anterior hippocampus was significantly increased in patients relative to controls ($p<0.01$).

Left anterior hippocampal diffusivity correlated negatively with FDG uptake in the left anterior hippocampus, left parahippocampal gyrus, right anterior hippocampus, right parahippocampal gyrus and the PCC [mostly its retrosplenial part; Brodmann area (BA) 29/30]; see Fig. 2 and Table 1. All clusters also survived a height threshold of $p<0.001$ uncorrected. The correlation analysis between right anterior hippocampal diffusivity and relative FDG uptake produced only a small cluster of significance (18 voxels, i.e. below our significance threshold for cluster extent) in the right parahippocampal gyrus. Lowering the p threshold to $p<0.05$ uncorrected revealed clusters of the same pattern as that obtained in the correlation with left anterior hippocampal diffusivity, albeit with the most significant clusters being located in the right hemisphere (see Fig. 2 and Table 1). No significant correlations between left or right posterior hippocampal diffusivity measurements and FDG uptake were noted.

As the pattern of the correlations for left and right anterior hippocampal diffusivity was nearly identical, but the associations were stronger in the former case, only significant clusters from the first correlation were considered for further analyses. Specifically, individual mean values from those three clusters (Table 1) were extracted and subsequently used for the correlation and logistic regression analyses. According to the location of the three significant clusters, FDG uptake was in addition extracted from the (entire) hippocampus, parahippocampal gyrus and the PCC separately for each hemisphere. Like values from the clusters, these VOI-based measurements were subsequently correlated with performance on DVR.

Scores from the DVR correlated with left anterior hippocampal diffusivity (Pearson correlation coefficient $r=-0.74$, $p<0.0005$), FDG uptake in the PCC cluster ($r=0.72$, $p<0.0005$), left ($r=0.62$, $p=0.004$) and right ($r=0.56$, $p=0.010$) hippocampal-parahippocampal cluster (Fig. 2). All VOI-based measurements except the right PCC significantly correlated with the DVR scores, albeit weaker then cluster-based measurements, with rs ranging from 0.45 to 0.50 ($p<0.05$).

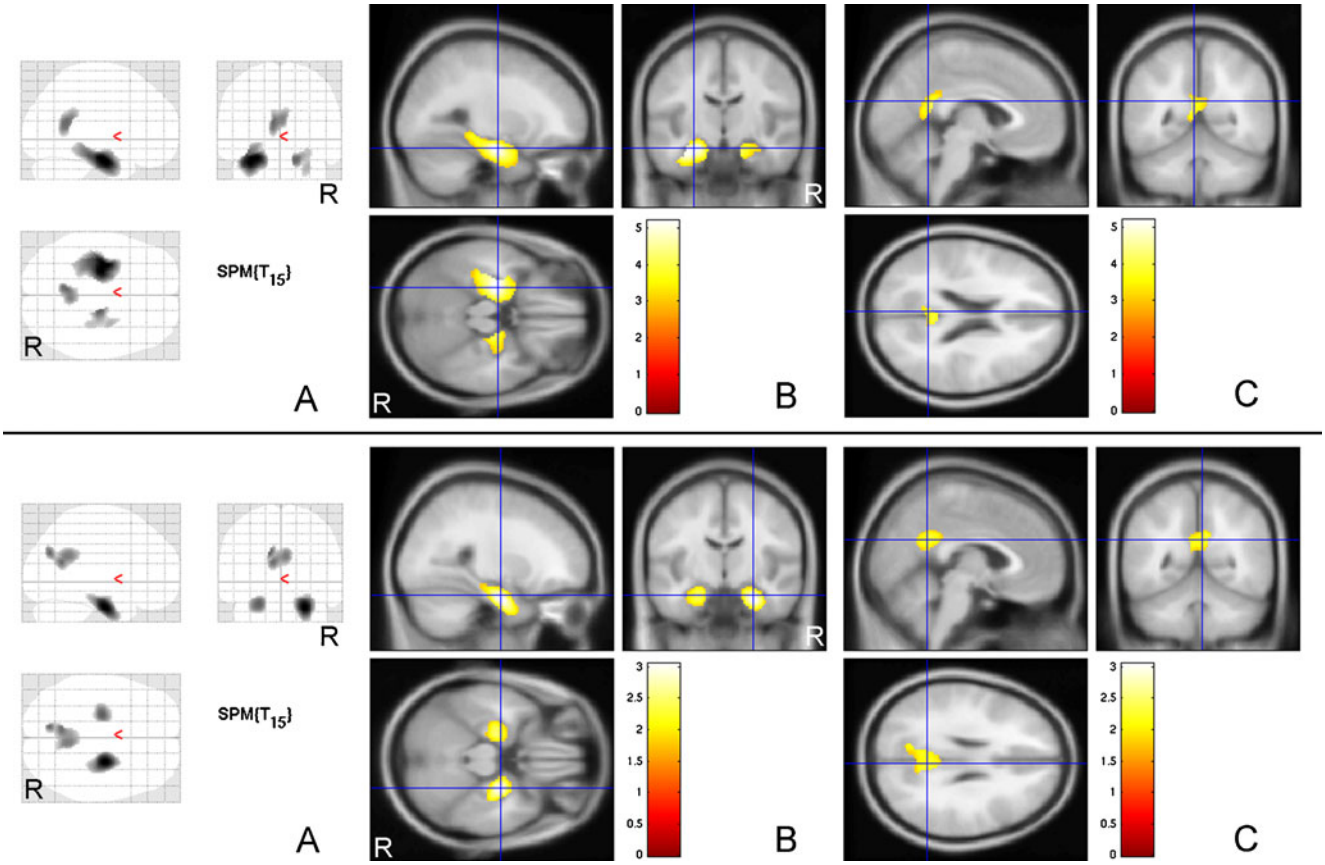

Fig. 2 SPM results of the partial (corrected for age, sex and education) negative correlation of left (*upper images*) and right (*lower images*) anterior hippocampal diffusivity with whole-brain FDG uptake in a sample of 20 patients with early Alzheimer's disease. Correlated regions are indicated as *dark clusters* projected onto glass brain (for viewing all significant findings) (**a**) and as *colour-coded clusters* projected onto sections of a standard MRI template (**b**, **c**). *Crossbars* indicate the location of significant voxel clusters in the hippocampus (**b**) and posterior cingulate (**c**); for coordinates see Table 1. Applied thresholds are $p<0.005$ (*upper images*) and $p<0.05$ (*lower images*) uncorrected for multiple comparisons, and $k>30$ voxels. *R* right, *L* left

Table 1 SPM results of the partial (corrected for age, sex and education) negative correlation of left ($p<0.005$ uncorrected) and right ($p<0.05$ uncorrected) anterior hippocampal diffusivity with whole-brain FDG uptake in a sample of 20 patients with early Alzheimer's disease

Diffusivity	Peak *t* value	Extent (voxels)	MNI coordinates			Anatomical structures
			x	y	z	
Left anterior hippocampus						
	5.19	1,736	−26	−12	−20	L (anterior) hippocampus, L parahippocampal gyrus (entorhinal, perirhinal, ectorhinal areas), L inferior temporal gyrus
	4.14	458	20	−14	−20	R parahippocampal gyrus (entorhinal area), R (anterior) hippocampus
	4.10	401	−4	−52	21	L and R posterior cingulate (retrosplenial, ventral areas)
Right anterior hippocampus						
	3.05	879	26	−10	−24	R (anterior) hippocampus, R parahippocampal gyrus (entorhinal, perirhinal areas)
	2.48	458	−21	−14	−24	L parahippocampal gyrus (entorhinal, perirhinal areas), L (anterior) hippocampus
	2.43	753	4	−52	26	R and L posterior cingulate (retrosplenial, ventral, dorsal areas)

R right, *L* left

In linear regression analyses, a stepwise procedure (default criteria, $P_{IN}=0.05$; $P_{OUT}=0.10$) revealed that diffusivity in the left anterior hippocampus was the strongest predictor of DVR performance ($R^2=51.5\%$, $p<0.0005$, $\beta=-0.74$), while FDG uptake in the PCC cluster significantly added to explained variance (R^2 change=+9.1%, $p=0.036$, $\beta=0.43$). The remaining predictors did not significantly increase the explained variance of the DVR.

Discussion

In the present study we explored the association between microstructural indices of the hippocampal integrity and voxel-wise maps of brain FDG utilization in early AD, also in relation to episodic memory impairment.

As the major finding, anterior hippocampal diffusivity correlated negatively with relative FDG uptake in the hippocampus, parahippocampal gyrus and the PCC, i.e. the major components of hippocampal output pathways. These structures also constitute critical nodes of the Papez circuit, which has an established role in the formation and retrieval of episodic memory. The specificity of the microstructural-metabolic associations is reinforced by a few lines of evidence. First, all the observed correlations were in the neurobiologically expected direction. Second, the detected metabolic correlations were in accord with the anatomy of the Papez circuit [13], i.e. only regions within the circuit were parts of the correlation pattern. Notably, not the entire PCC, but specifically the *retrosplenial* cortex (BA29/30) was consistently involved in all significant correlations. This posterior cingulate subregion receives a direct innervation from the hippocampal formation via the cingulate bundle [8, 30]. Third, the peak correlations were observed ipsilateral to the hippocampal diffusivity changes, i.e. left hippocampal diffusivity correlated most strongly with regional FDG uptake in the left hemisphere. Importantly, a nearly identical pattern of the correlations was found in the right hemisphere. Although the correlation on the right side was most evident at a lower threshold, the consistent bilateral pattern of correlations supports the overall robustness of the established relationships.

As mentioned above, disturbed connectivity between the hippocampal formation and the PCC has been proposed as the mechanism behind PCC hypometabolism and perfusion in AD [4, 5]. In view of the anatomical studies cited above, the diaschisis is likely to be related to disruption of the cingulate bundle, along with the fornix, the major pathway constituting the Papez circuit [31]. Indeed, degenerative alterations of this white matter tract in AD have been documented in a number of studies [19, 32, 33]. Chételat et al. (2008) compared regional effects of atrophy and hypometabolism in AD and found that regions showing the most significant predominance of hypometabolism were those connected to the hippocampus via the cingulate bundle [6]. At the neuronal level, anterograde Wallerian degeneration of the cingulate bundle fibres originating in the hippocampal formation may well be the underlying mechanism of the diaschisis [34, 35]. In line with this view, very recent evidence indicates that cingulum fibre disruption begins near medial temporal structures and then proceeds to the PCC with AD progression from the preclinical to clinically evident stage [36]. Furthermore, a path of interest analysis of the parahippocampal white matter that includes the cingulate bundle indicates an anterior to posterior gradient of AD-related damage with stronger degenerative alterations in the more anterior portions [37]. Such an ascending course of cingulum bundle degeneration is indirectly supported here by the observation that the correlation's strength declined in the order hippocampus>parahippocampal gyrus>PCC.

The second major finding of this study was that glucose metabolism in the regions involved in the association with hippocampal diffusivity, particularly the retrosplenial cortex, was strongly related to functional performance in our subjects with early AD. Herewith the present work implicates the dysfunction of structures along the hippocampal output pathways as a significant factor in the genesis of episodic memory impairment in AD. Although correlation does not mean causality, we hypothesize that hippocampal damage as measured by increased anterior hippocampal diffusivity in our subjects with early AD was the initiator of the observed metabolic and functional alterations. The resulting diaschisis phenomenon affected functioning of the associated regions including posterior parts of the PCC, which in turn exacerbated episodic memory impairment. Indeed, there are converging lines of evidence that the PCC or, more specifically, the retrosplenial cortex plays an important role in episodic memory. Focal lesions to the retrosplenial cortex cause amnesia in humans [38–40] and, as shown by fMRI studies, this brain region is consistently activated during episodic memory retrieval (for a review see [41]). Furthermore, episodic memory performance correlates with glucose metabolism in the retrosplenial cortex and parahippocampal gyrus in subjects with mild AD [42]. Consistently, our additional VOI-based analysis indicated that specifically the retrosplenial cortex rather than entire PCC predicted performance on DVR.

A further important finding of our study was that the anterior part of the hippocampus, rather than the whole structure, was specifically involved in the above reported microstructural-metabolic correlations. Evidence for a

functional differentiation of the hippocampus along its longitudinal axis has been discussed in detail previously [20, 43, 44]. The principal input from multimodal association neocortical areas occurs mainly through the anterior hippocampus by means of the perforant path that arises in the entorhinal cortex [45]. Numerous lesion studies in experimental animals (e.g. [46]) show that integrity of the perforant path is a major prerequisite for normal memory function (for review see [47]), and disruption of this path, as is known to occur very early in the course of AD, produces profound memory impairment in humans [48–50]. The specific role of the perforant path in memory function was recently supported by in vivo neuroimaging studies in patients with MCI and AD [51, 52].

We found that the microstructural-metabolic correlations were substantially weaker in the right hemisphere, even though hippocampal diffusivity changes were rather symmetric [20]. This observation suggests involvement of other factors in the regional metabolic impairment in addition to hippocampal damage such as other connectivity (e.g. reorganization of neuronal circuits) [53] or specific local processes, e.g. amyloid deposition [54] or oxidative damage [55]. Of note, the PCC is particularly vulnerable to amyloid deposition, which occurs in this region very early in the course of AD [54, 56]. Moreover, a very recent multimodal imaging study reported the presence of subtle connectivity disruption and PCC hypometabolism even in asymptomatic amyloid-positive elderly subjects [57]. Laterality and asymmetry of amyloid deposition was evaluated by Raji and colleagues [58]. Interestingly, they observed a rightward (i.e. right more than left), although not significant, asymmetry in amyloid deposition in the structures of the medial temporal lobe and precuneus in patients with AD; the PCC was, however, not examined in that study. Furthermore, it might be argued that possible structural changes in the PCC of patients with AD [36, 59] could have driven the present association with relative FDG uptake. Consequently, we carried out an additional partial correlation analysis with PCC volume and PCC diffusivity, both estimated from the above probabilistic atlas [27, 28], entered as nuisance variables. However, this approach did not substantially influence the correlation pattern (data not shown), thus supporting the overall robustness of our findings. Nevertheless, it should be clearly noted that, like previous studies on this issue [12, 14], our cross-sectional investigation only establishes a relationship between hippocampal degeneration and regional metabolic dysfunction, but does not clarify which phenomenon occurs first. Furthermore, there can be no doubt that the diaschisis is not the only cause of regional metabolic deterioration, but there are other factors (see above) that substantially contribute to functionally relevant metabolic deficits.

Conclusion

In conclusion, we found a significant association between anterior hippocampal diffusivity and FDG uptake in the hippocampus, parahippocampal gyrus and the PCC in patients with early AD. These regions are connected by the cingulate bundle and constitute major components of the Papez circuit, which subserves episodic memory. Accordingly, glucose metabolism in the PCC, along with anterior hippocampal diffusivity, significantly predicted episodic memory performance in our patients with early AD. Our data support the diaschisis hypothesis of AD and implicate the diaschisis phenomenon as a significant factor in the genesis of episodic memory impairment in AD.

Conflicts of interest None.

References

1. Braak H, Braak E. Neuropathological stageing of Alzheimer-related changes. Acta Neuropathol 1991;82:239–59.
2. Gainotti G, Marra C, Villa G, Parlato V, Chiarotti F. Sensitivity and specificity of some neuropsychological markers of Alzheimer dementia. Alzheimer Dis Assoc Disord 1998;12:152–62.
3. de Leon MJ, Mosconi L, Blennow K, DeSanti S, Zinkowski R, Mehta PD, et al. Imaging and CSF studies in the preclinical diagnosis of Alzheimer's disease. Ann N Y Acad Sci 2007;1097:114–45.
4. Minoshima S, Giordani B, Berent S, Frey KA, Foster NL, Kuhl DE. Metabolic reduction in the posterior cingulate cortex in very early Alzheimer's disease. Ann Neurol 1997;42:85–94.
5. Kogure D, Matsuda H, Ohnishi T, Asada T, Uno M, Kunihiro T, et al. Longitudinal evaluation of early Alzheimer's disease using brain perfusion SPECT. J Nucl Med 2000;41:1155–62.
6. Chételat G, Desgranges B, Landeau B, Mézenge F, Poline JB, de la Sayette V, et al. Direct voxel-based comparison between grey matter hypometabolism and atrophy in Alzheimer's disease. Brain 2008;131:60–71.
7. Meguro K, Blaizot X, Kondoh Y, Le Mestric C, Baron JC, Chavoix C. Neocortical and hippocampal glucose hypometabolism following neurotoxic lesions of the entorhinal and perirhinal cortices in the non-human primate as shown by PET. Implications for Alzheimer's disease. Brain 1999;122:1519–31.
8. Kobayashi Y, Amaral DG. Macaque monkey retrosplenial cortex: II. Cortical afferents. J Comp Neurol 2003;466:48–79.
9. Schmahmann JD, Pandya DN, Wang R, Dai G, D'Arceuil HE, de Crespigny AJ, et al. Association fibre pathways of the brain: parallel observations from diffusion spectrum imaging and autoradiography. Brain 2007;130:630–53.
10. Mori S, Wakana S, Van Zijl PCM, Nagae-Poetscher LM, editors. MRI atlas of human white matter. Oxford: Elsevier Ltd.; 2005.
11. Machado CJ, Snyder AZ, Cherry SR, Lavenex P, Amaral DG. Effects of neonatal amygdala or hippocampus lesions on resting brain metabolism in the macaque monkey: a microPET imaging study. Neuroimage 2008;39:832–46.
12. Villain N, Desgranges B, Viader F, de la Sayette V, Mézenge F, Landeau B, et al. Relationships between hippocampal atrophy, white matter disruption, and gray matter hypometabolism in Alzheimer's disease. J Neurosci 2008;28:6174–81.

13. Papez J. A proposed mechanism of emotion. Arch Neurol Psychiatry 1937;38:725–43.
14. Guedj E, Barbeau EJ, Didic M, Felician O, de Laforte C, Ranjeva JP, et al. Effects of medial temporal lobe degeneration on brain perfusion in amnestic MCI of AD type: deafferentation and functional compensation? Eur J Nucl Med Mol Imaging 2009;36:1101–12.
15. Petersen RC, Stevens JC, Ganguli M, Tangalos EG, Cummings JL, DeKosky ST. Practice parameter: early detection of dementia: mild cognitive impairment (an evidence-based review). Report of the Quality Standards Subcommittee of the American Academy of Neurology. Neurology 2001;56:1133–42.
16. Basser PJ, Pierpaoli C. Microstructural and physiological features of tissues elucidated by quantitative-diffusion-tensor MRI. J Magn Reson B 1996;111:209–19.
17. Kantarci K, Petersen RC, Boeve BF, Knopman DS, Weigand SD, O'Brien PC. DWI predicts future progression to Alzheimer disease in amnestic mild cognitive impairment. Neurology 2005;64:902–4.
18. Müller MJ, Greverus D, Weibrich C, Dellani PR, Scheurich A, Stoeter P, et al. Diagnostic utility of hippocampal size and mean diffusivity in amnestic MCI. Neurobiol Aging 2007;28:398–403.
19. Zhang Y, Schuff N, Jahng GH, Bayne W, Mori S, Schad L, et al. Diffusion tensor imaging of cingulum fibers in mild cognitive impairment and Alzheimer disease. Neurology 2007;68:13–9.
20. Yakushev I, Müller MJ, Lorscheider M, Schermuly I, Weibrich C, Dellani PR, et al. Increased hippocampal head diffusivity predicts impaired episodic memory performance in early Alzheimer's disease. Neuropsychologia 2010;48:1447–53.
21. Yakushev I, Bartenstein P, Siessmeier T, Hiemke C, Scheurich A, Lotz J, et al. Cerebrospinal fluid tau protein levels and 18F-fluorodeoxyglucose positron emission tomography in the differential diagnosis of Alzheimer's disease. Dement Geriatr Cogn Disord 2010;30:245–53.
22. Dubois B, Feldman HH, Jacova C, Dekosky ST, Barberger-Gateau P, Cummings J, et al. Research criteria for the diagnosis of Alzheimer's disease: revising the NINCDS-ADRDA criteria. Lancet Neurol 2007;6:734–46.
23. Welsh KA, Butters N, Mohs RC, Beekly D, Edland S, Fillenbaum G, et al. The Consortium to Establish a Registry for Alzheimer's Disease (CERAD). Part V. A normative study of the neuropsychological battery. Neurology 1994;44:609–14.
24. Basser PJ, Mattiello J, LeBihan D. Estimation of the effective self-diffusion tensor from the NMR spin echo. J Magn Reson B 1994;103:247–54.
25. Yakushev I, Landvogt C, Buchholz HG, Fellgiebel A, Hammers A, Scheurich A, et al. Choice of reference area in studies of Alzheimer's disease using positron emission tomography with fluorodeoxyglucose-F18. Psychiatry Res 2008;164:143–53.
26. Yakushev I, Hammers A, Fellgiebel A, Schmidtmann I, Scheurich A, Buchholz HG, et al. SPM-based count normalization provides excellent discrimination of mild Alzheimer's disease and amnestic mild cognitive impairment from healthy aging. Neuroimage 2009;44:43–50.
27. Hammers A, Allom R, Koepp MJ, Free SL, Myers R, Lemieux L, et al. Three-dimensional maximum probability atlas of the human brain, with particular reference to the temporal lobe. Hum Brain Mapp 2003;19:224–47.
28. Gousias IS, Rueckert D, Heckemann RA, Dyet LE, Boardman JP, Edwards AD, et al. Automatic segmentation of brain MRIs of 2-year-olds into 83 regions of interest. Neuroimage 2008;40:672–84.
29. Edison P, Archer HA, Hinz R, Hammers A, Pavese N, Tai YF, et al. Amyloid, hypometabolism, and cognition in Alzheimer disease: an [11C]PIB and [18F]FDG PET study. Neurology 2007;68:501–8.
30. Kobayashi Y, Amaral DG. Macaque monkey retrosplenial cortex: III. Cortical efferents. J Comp Neurol 2007;502:810–33.
31. Concha L, Gross DW, Beaulieu C. Diffusion tensor tractography of the limbic system. AJNR Am J Neuroradiol 2005;26:2267–74.
32. Fellgiebel A, Müller MJ, Wille P, Dellani PR, Scheurich A, Schmidt LG, et al. Color-coded diffusion-tensor-imaging of posterior cingulate fiber tracts in mild cognitive impairment. Neurobiol Aging 2005;26:1193–8.
33. Teipel SJ, Born C, Ewers M, Bokde ALW, Reiser MF, Möller HJ, et al. Multivariate deformation-based analysis of brain atrophy to predict Alzheimer's disease in mild cognitive impairment. Neuroimage 2007;38:13–24.
34. Scheltens P, Barkhof F, Leys D, Wolters EC, Ravid R, Kamphorst W. Histopathologic correlates of white matter changes on MRI in Alzheimer's disease and normal aging. Neurology 1995;45:883–8.
35. Huang J, Friedland RP, Auchus AP. Diffusion tensor imaging of normal-appearing white matter in mild cognitive impairment and early Alzheimer disease: preliminary evidence of axonal degeneration in the temporal lobe. AJNR Am J Neuroradiol 2007;28:1943–8.
36. Choo IH, Lee DY, Oh JS, Lee JS, Lee DS, Song IC, et al. Posterior cingulate cortex atrophy and regional cingulum disruption in mild cognitive impairment and Alzheimer's disease. Neurobiol Aging 2010;31:772–9.
37. Salat DH, Tuch DS, van der Kouwe AJW, Greve DN, Pappu V, Lee SY, et al. White matter pathology isolates the hippocampal formation in Alzheimer's disease. Neurobiol Aging 2010;31:244–56.
38. Valenstein E, Bowers D, Verfaellie M, Heilman KM, Day A, Watson RT. Retrosplenial amnesia. Brain 1987;110:1631–46.
39. Maguire EA. The retrosplenial contribution to human navigation: a review of lesion and neuroimaging findings. Scand J Psychol 2001;42:225–38.
40. McDonald CR, Crosson B, Valenstein E, Bowers D. Verbal encoding deficits in a patient with a left retrosplenial lesion. Neurocase 2001;7:407–17.
41. Wagner AD, Shannon BJ, Kahn I, Buckner RL. Parietal lobe contributions to episodic memory retrieval. Trends Cogn Sci 2005;9:445–53.
42. Desgranges B, Baron JC, Lalevée C, Giffard B, Viader F, de La Sayette V, et al. The neural substrates of episodic memory impairment in Alzheimer's disease as revealed by FDG-PET: relationship to degree of deterioration. Brain 2002;125:1116–24.
43. Witter MP. The perforant path: projections from the entorhinal cortex to the dentate gyrus. Prog Brain Res 2007;163:43–61.
44. Yakushev I, Fellgiebel A. Horizontal versus longitudinal axis of the hippocampus: metabolic differentiation as measured with high-resolution PET/MRI. J Nucl Med 2011;52:329.
45. Hyman BT, Van Hoesen GW, Damasio AR, Barnes CL. Alzheimer's disease: cell-specific pathology isolates the hippocampal formation. Science 1984;225:1168–70.
46. Kirkby DL, Higgins GA. Characterization of perforant path lesions in rodent models of memory and attention. Eur J Neurosci 1998;10:823–38.
47. Rolls ET. An attractor network in the hippocampus: theory and neurophysiology. Learn Mem 2007;14:714–31.
48. Hyman BT, Van Hoesen GW, Kromer LJ, Damasio AR. Perforant pathway changes and the memory impairment of Alzheimer's disease. Ann Neurol 1986;20:472–81.
49. Shukla C, Bridges LR. Tau, beta-amyloid and beta-amyloid precursor protein distribution in the entorhinal-hippocampal alvear and perforant pathways in the Alzheimer's brain. Neurosci Lett 2001;303:193–7.

50. García-Sierra F, Hauw JJ, Duyckaerts C, Wischik CM, Luna-Muñoz J, Mena R. The extent of neurofibrillary pathology in perforant pathway neurons is the key determinant of dementia in the very old. Acta Neuropathol 2000;100:29–35.
51. Kalus P, Slotboom J, Gallinat J, Mahlberg R, Cattapan-Ludewig K, Wiest R, et al. Examining the gateway to the limbic system with diffusion tensor imaging: the perforant pathway in dementia. Neuroimage 2006;30:713–20.
52. Stoub TR, deToledo-Morrell L, Stebbins GT, Leurgans S, Bennett DA, Shah RC. Hippocampal disconnection contributes to memory dysfunction in individuals at risk for Alzheimer's disease. Proc Natl Acad Sci U S A 2006;103:10041–5.
53. Deller T, Haas CA, Freiman TM, Phinney A, Jucker M, Frotscher M. Lesion-induced axonal sprouting in the central nervous system. Adv Exp Med Biol 2006;557:101–21.
54. Forsberg A, Engler H, Almkvist O, Blomquist G, Hagman G, Wall A, et al. PET imaging of amyloid deposition in patients with mild cognitive impairment. Neurobiol Aging 2008;29:1456–65.
55. Mosconi L, Pupi A, De Leon MJ. Brain glucose hypometabolism and oxidative stress in preclinical Alzheimer's disease. Ann N Y Acad Sci 2008;1147:180–95.
56. Small GW, Kepe V, Ercoli LM, Siddarth P, Bookheimer SY, Miller KJ, et al. PET of brain amyloid and tau in mild cognitive impairment. N Engl J Med 2006;355:2652–63.
57. Drzezga A, Becker JA, Van Dijk KR, Sreenivasan A, Talukdar T, Sullivan C, et al. Neuronal dysfunction and disconnection of cortical hubs in non-demented subjects with elevated amyloid burden. Brain 2011;134:1635–46. doi:10.1093/brain/awr066.
58. Raji CA, Becker JT, Tsopelas ND, Price JC, Mathis CA, Saxton JA, et al. Characterizing regional correlation, laterality and symmetry of amyloid deposition in mild cognitive impairment and Alzheimer's disease with Pittsburgh Compound B. J Neurosci Methods 2008;172:277–82.
59. Pengas G, Hodges JR, Watson P, Nestor PJ. Focal posterior cingulate atrophy in incipient Alzheimer's disease. Neurobiol Aging 2010;31:25–33.